Hybrid phase-change plasmonic crystals for active tuning of lattice resonances

Y. G. Chen,[1-3] T. S. Kao,[1] B. Ng,[3] X. Li,[4] X. G. Luo,[4] B. Luk'yanchuk,[2] S. A. Maier,[3] and M. H. Hong[1,*]

[1]*Department of Electrical and Computer Engineering, National University of Singapore, 4 Engineering Drive 3, 117576 Singapore*

[2]*Data Storage Institute, (A*STAR) Agency for Science Technology and Research, 5 Engineering Drive 1, 117608 Singapore*

[3]*Experimental Solid State Group, Physics Department, Imperial College London, London SW7 2AZ, UK*

[4]*State Key Laboratory of Optical Technologies on Nano-Fabrication and Micro-Engineering, Institute of Optics and Electronics, Chinese Academy of Science, P.O.box 350, Chengdu 610209, China*

**elehmh@nus.edu.sg*

Abstract: Tunable lattice resonances are demonstrated in a hybrid plasmonic crystal incorporating the phase-change material $Ge_2Sb_2Te_5$ (GST) as a 20-nm-thick layer sandwiched between a gold nanodisk array and a quartz substrate. Non-volatile tuning of lattice resonances over a range $\Delta\lambda$ of about 500 nm (1.89 μm to 2.27 μm) is achieved experimentally via intermediate phase states of the GST layer. This work demonstrates the efficacy and ease of resonance tuning via GST in the near infrared, suggesting the possibility to design broadband non-volatile tunable devices for optical modulation, switching, sensing and nonlinear optical devices.

OCIS codes: (260.5740) Resonance; (240.6680) Surface plasmons; (310.6845) Thin film devices and applications; (350.2770) Gratings.

References and Links

1. B. Ng, S. M. Hanham, V. Giannini, Z. C. Chen, M. Tang, Y. F. Liew, N. Klein, M. H. Hong, and S. A. Maier, "Lattice resonances in antenna arrays for liquid sensing in the terahertz regime," Opt. Express **19**(15), 14653–14661 (2011).
2. G. Vecchi, V. Giannini, and J. Gómez Rivas, "Shaping the fluorescent emission by lattice resonances in plasmonic crystals of nanoantennas," Phys. Rev. Lett. **102**(14), 146807 (2009).
3. E. M. Hicks, S. Zou, G. C. Schatz, K. G. Spears, R. P. Van Duyne, L. Gunnarsson, T. Rindzevicius, B. Kasemo, and M. Käll, "Controlling plasmon line shapes through diffractive coupling in linear arrays of cylindrical nanoparticles fabricated by electron beam lithography," Nano Lett. **5**(6), 1065–1070 (2005).
4. J. Y. Ou, E. Plum, J. Zhang, and N. I. Zheludev, "An electromechanically reconfigurable plasmonic metamaterial operating in the near-infrared," Nat. Nanotechnol. **8**(4), 252–255 (2013).
5. J. Y. Ou, E. Plum, L. Jiang, and N. I. Zheludev, "Reconfigurable photonic metamaterials," Nano Lett. **11**(5), 2142–2144 (2011).
6. Y. Cui, J. Zhou, V. A. Tamma, and W. Park, "Dynamic tuning and symmetry lowering of Fano resonance in plasmonic nanostructure," ACS Nano **6**(3), 2385–2393 (2012).
7. H. Tao, A. C. Strikwerda, K. Fan, W. J. Padilla, X. Zhang, and R. D. Averitt, "Reconfigurable terahertz metamaterials," Phys. Rev. Lett. **103**(14), 147401 (2009).
8. I. M. Pryce, K. Aydin, Y. A. Kelaita, R. M. Briggs, and H. A. Atwater, "Highly strained compliant optical metamaterials with large frequency tunability," Nano Lett. **10**(10), 4222–4227 (2010).
9. H. T. Chen, W. J. Padilla, J. M. O. Zide, A. C. Gossard, A. J. Taylor, and R. D. Averitt, "Active terahertz metamaterial devices," Nature **444**(7119), 597–600 (2006).
10. J. Gu, R. Singh, X. Liu, X. Zhang, Y. Ma, S. Zhang, S. A. Maier, Z. Tian, A. K. Azad, H. T. Chen, A. J. Taylor, J. Han, and W. Zhang, "Active control of electromagnetically induced transparency analogue in terahertz metamaterials," Nat Commun **3**, 1151 (2012).
11. T. Driscoll, S. Palit, M. M. Qazilbash, M. Brehm, F. Keilmann, B. G. Chae, S. J. Yun, H. T. Kim, S. Y. Cho, N. M. Jokerst, D. R. Smith, and D. N. Basov, "Dynamic tuning of an infrared hybrid-metamaterial resonance using vanadium dioxide," Appl. Phys. Lett. **93**(2), 024101 (2008).
12. D. Loke, T. H. Lee, W. J. Wang, L. P. Shi, R. Zhao, Y. C. Yeo, T. C. Chong, and S. R. Elliott, "Breaking the speed limits of phase-change memory," Science **336**(6088), 1566–1569 (2012).

#189457 - $15.00 USD Received 25 Apr 2013; revised 23 May 2013; accepted 25 May 2013; published 31 May 2013

13. J.-W. Park, S. H. Baek, T. D. Kang, H. Lee, Y.-S. Kang, T.-Y. Lee, D.-S. Suh, K. J. Kim, C. K. Kim, Y. H. Khang, J. L. F. Da Silva, and S.-H. Wei, "Optical properties of (GeTe, Sb2Te3) pseudobinary thin films studied with spectroscopic ellipsometry," Appl. Phys. Lett. **93**(2), 021914 (2008).
14. T. Driscoll, H. T. Kim, B. G. Chae, B. J. Kim, Y. W. Lee, N. M. Jokerst, S. Palit, D. R. Smith, M. Di Ventra, and D. N. Basov, "Memory metamaterials," Science **325**(5947), 1518–1521 (2009).
15. M. J. Dicken, K. Aydin, I. M. Pryce, L. A. Sweatlock, E. M. Boyd, S. Walavalkar, J. Ma, and H. A. Atwater, "Frequency tunable near-infrared metamaterials based on VO_2 phase transition," Opt. Express **17**(20), 18330–18339 (2009).
16. K. Appavoo, D. Y. Lei, Y. Sonnefraud, B. Wang, S. T. Pantelides, S. A. Maier, and R. F. Haglund, Jr., "Role of defects in the phase transition of VO_2 nanoparticles probed by plasmon resonance spectroscopy," Nano Lett. **12**(2), 780–786 (2012).
17. D. Y. Lei, K. Appavoo, Y. Sonnefraud, R. F. Haglund, Jr., and S. A. Maier, "Single-particle plasmon resonance spectroscopy of phase transition in vanadium dioxide," Opt. Lett. **35**(23), 3988–3990 (2010).
18. H. Verleur, A. B. Jr, and C. Berglund, "Optical properties of VO_2 between 0.25 and 5 eV," Phys. Rev. **172**(3), 788–798 (1968).
19. N. Yamada, M. Otoba, K. Kawahara, N. Miyagawa, H. Ohta, N. Akahira, and T. Matsunaga, "Phase-change optical disk having a nitride interface layer," Jpn. J. Appl. Phys. **37**(Part 1, No. 4B), 2104–2110 (1998).
20. N. Yamada, "Development of materials for third generation optical storage media," in *Phase Change Materials: Science and Applications*, S. Raoux and M. Wuttig, eds. (Springer, 2009).
21. C. H. Chu, C. D. Shiue, H. W. Cheng, M. L. Tseng, H.-P. Chiang, M. Mansuripur, and D. P. Tsai, "Laser-induced phase transitions of $Ge_2Sb_2Te_5$ thin films used in optical and electronic data storage and in thermal lithography," Opt. Express **18**(17), 18383–18393 (2010).
22. C. M. Chang, C. H. Chu, M. L. Tseng, H. P. Chiang, M. Mansuripur, and D. P. Tsai, "Local electrical characterization of laser-recorded phase-change marks on amorphous $Ge_2Sb_2Te_5$ thin films," Opt. Express **19**(10), 9492–9504 (2011).
23. M. L. Tseng, B. H. Chen, C. H. Chu, C. M. Chang, W. C. Lin, N. N. Chu, M. Mansuripur, A. Q. Liu, and D. P. Tsai, "Fabrication of phase-change chalcogenide $Ge_2Sb_2Te_5$ patterns by laser-induced forward transfer," Opt. Express **19**(18), 16975–16984 (2011).
24. P. K. Khulbe, E. M. Wright, and M. Mansuripur, "Crystallization behavior of as-deposited, melt quenched, and primed amorphous states of $Ge_2Sb_{2.3}Te_5$ films," J. Appl. Phys. **88**(7), 3926–3933 (2000).
25. L. Shi, T. Chong, P. K. Tan, X. S. Miao, Y. M. Huang, and R. Zhao, "Study of the partial crystallization properties of phase-change optical recording disks," J. Appl. Phys. **38**, 1645–1648 (1999).
26. B. Auguié and W. L. Barnes, "Collective resonances in gold nanoparticle arrays," Phys. Rev. Lett. **101**(14), 143902 (2008).
27. H. Li, X. Luo, C. Du, X. Chen, and Y. Fu, "Ag dots array fabricated using laser interference technique for biosensing," Sens. Actuators B Chem. **134**(2), 940–944 (2008).
28. Z. L. Sámson, K. F. MacDonald, F. De Angelis, B. Gholipour, K. Knight, C. C. Huang, E. Di Fabrizio, D. W. Hewak, and N. I. Zheludev, "Metamaterial electro-optic switch of nanoscale thickness," Appl. Phys. Lett. **96**(14), 143105 (2010).
29. U. Russo, D. Ielmini, and A. Lacaita, "Analytical modeling of chalcogenide crystallization for PCM data-retention extrapolation," IEEE Trans. Electron. Dev. **54**(10), 2769–2777 (2007).
30. N. V. Voshchinnikov, G. Videen, and T. Henning, "Effective medium theories for irregular fluffy structures: aggregation of small particles," Appl. Opt. **46**(19), 4065–4072 (2007).
31. D. Aspnes, "Local-field effects and effective-medium theory: A microscopic perspective," Am. J. Phys. **50**(8), 704–709 (1982).
32. V. Weidenhof, I. Friedrich, S. Ziegler, and M. Wuttig, "Atomic force microscopy study of laser induced phase transitions in $Ge_2Sb_2Te_5$," J. Appl. Phys. **86**(10), 5879–5887 (1999).
33. M. Wuttig, D. Lüsebrink, D. Wamwangi, W. Wełnic, M. Gillessen, and R. Dronskowski, "The role of vacancies and local distortions in the design of new phase-change materials," Nat. Mater. **6**(2), 122–128 (2007).
34. L. Gross, R. R. Schlittler, G. Meyer, A. Vanhaverbeke, and R. Allenspach, "Fabrication of ultrathin magnetic structures by nanostencil lithography in dynamic mode," Appl. Phys. Lett. **90**(9), 093121 (2007).
35. P. Němec, A. Moreac, V. Nazabal, M. Pavlišta, J. Přikryl, and M. Frumar, "Ge–Sb–Te thin films deposited by pulsed laser: An ellipsometry and Raman scattering spectroscopy study," J. Appl. Phys. **106**(10), 103509 (2009).
36. G. Vecchi, V. Giannini, and J. Gómez Rivas, "Surface modes in plasmonic crystals induced by diffractive coupling of nanoantennas," Phys. Rev. B **80**(20), 201401 (2009).

1. Introduction

Lattice resonances, the diffractive coupling of light to localized surface plasmon resonances (LSPRs) in plasmonic crystals, are much narrower than conventional dipolar LSPRs and have interesting applications such as the modification of fluorescent emission and sensing [1–3]. Unfortunately, the lattice resonance frequency is fixed by geometric and material parameters [3]. This hinders the application of lattice resonances to practical devices, where real-time tunability of the resonance is desirable. Much research effort has been devoted to developing

#189457 - $15.00 USD Received 25 Apr 2013; revised 23 May 2013; accepted 25 May 2013; published 31 May 2013

methods to tune plasmonic resonances so that optical components with engineered optical responses and a large working frequency range can be realized [4–6]. Semiconductors-controlled carriers concentration modulation and geometric tuning based on micro-electro-mechanical systems (MEMs) have been applied to split-ring resonators (SRRs) [5,7–9] as well as to Fano-type metamaterials [10] to exhibit frequency-agile properties under external stimulus in the past. More recently, phase-change materials have emerged as a promising candidate for resonance tuning, due to their extreme phase switching speeds and the drastic changes in their optical properties upon phase change [11–13]. For example, vanadium dioxide (VO_2) hybrid metamaterials have been previously shown to have tunable resonances resulting from the VO_2 phase transition at THz and IR frequencies [11,14–17]. However, the resonance shifting effect is subtle at near infrared (NIR) frequencies because the complex refractive index ($n + ik$) of VO_2 changes only slightly in n but significantly in k during the phase transition [18].

$Ge_2Sb_2Te_5$ (GST) is a phase-change material that has been widely used in commercial optical disks and phase-change memory. GST has many attractive intrinsic properties including its large complex refractive index contrast between crystalline and amorphous phases, short tuning time (less than 30 ns), high stability in room temperature, and large cycle number [19,20]. Changing the phase state of GST can be easily realized through mature methods such as the application of an electric current, optical pumping and thermal stimulus [21,22]. By precisely controlling the energy and duration of the stimulus, multi-state structures can be engineered with the phase state of GST tuned to the designed crystallization level [23–25]. In the NIR, a drastic change in the real part of the refractive index from the phase transition and moderately low absorptive losses allow GST to significantly alter the dielectric environment of the resonator while keeping losses manageable. These properties make GST a suitable candidate for achieving a tunable lattice resonance in the NIR within the environment of a plasmonic crystal.

In this article, hybrid phase-change plasmonic crystals used for tuning lattice resonances over a broad spectral range are demonstrated. The GST layer is sandwiched between a gold nanodisk array and a quartz substrate and acts as a tunable dielectric environment for the nanodisk array. The advantage of using a GST tuning layer is its large refractive index contrast, ease of inducing phase transitions and the ability to access intermediate states consisting of a mix of both amorphous and crystalline GST. Here we demonstrate lattice resonance tuning in the NIR regime of the spectrum with shifts on the order of 500 nm.

2. Sample design and simulation

Figure 1(a) schematically shows the layer structure of a hybrid phase-change plasmonic crystal which consists of a gold nanodisks array and an underneath thin film of GST. The nanodisks, with a dimension of 280 nm in diameter and 40 nm in thickness, are arranged in square lattice with a period of 1.2 μm. The GST thin film underneath the nanodisks is 20 nm thick.

The simulation results in this work were obtained by the finite-difference-time-domain (FDTD) method (FDTD Solutions 7.5, Lumerical Inc.). A broadband plane wave in z direction was used to excite the structure. Periodic boundary conditions were applied to a unit cell in x and y directions. The optical constants of GST were obtained from [20].

#189457 - $15.00 USD Received 25 Apr 2013; revised 23 May 2013; accepted 25 May 2013; published 31 May 2013

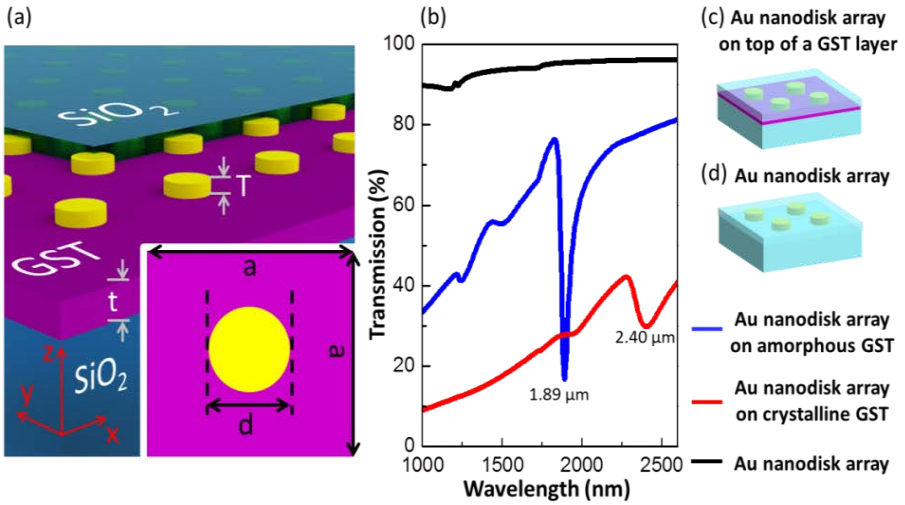

Fig. 1. (a) Schematic diagram of the GST-Au hybrid plasmonic crystal (T = 40 nm, t = 20 nm, d = 280 nm, a = 1.2 μm). A GST phase-change thin film underneath an array of gold nanodisks is used for controlling the resonant frequencies. (b) Simulated transmission spectra of plasmonic crystals with the GST layer in amorphous and crystalline phases, and a plasmonic crystal without underneath GST. The three spectra are denoted in blue, red and black colors, respectively. Configurations of plasmonic crystals with the underneath GST layer and without the GST layer are illustrated in (c) and (d).

Figure 1(b) shows the comparisons between the simulated far-field transmission spectra of plasmonic crystals with three sample configurations: a hybrid phase-change plasmonic crystal with a GST thin layer in amorphous and crystalline phases as shown in Fig. 1(c), and a gold nanodisk array on a quartz substrate as shown in Fig. 1(d). Regarding the Au nanodisk array on a quartz substrate, the spectrum (black curve) shows that no significant lattice resonance mode is generated, indicating a weak coupling between the diffractive modes and the dipole resonance of individual nanodisk [26]. In the hybrid phase-change plasmonic crystal with a GST thin film in the amorphous phase, a collective mode from the periodicity of constituent nanodisks and the interaction between the dipoles can occur, generating a sharp lattice resonance at the wavelength of 1.89 μm as the black curve shown in Fig. 1(b). The Q-factor, bandwidth relative to its center frequency of this resonance dip is around 17. Switching the GST thin film to crystalline phase, the resonance feature is red-shifted to the wavelength of 2.40 μm with a shallower resonance dip and the Q-factor is around 13. This shallower resonance dip may result from more metal-like optical properties associated with the crystalline GST thin film, which leads to an enhanced absorption and reflection thus decreasing the transmitted light intensity. As can be seen in Fig. 1(b), the significant shift in resonance would result in a large modulation of the transmitted light intensity, for example, the transmittance difference at the wavelength of 2.40 μm is about 50%.

3. Experimental

To fabricate the samples, the laser interference lithography (LIL) with dry etching was used. The fabrication process of this plasmonic crystal is described in Fig. 2(a). To start with this process, an as-deposited GST thin layer of designed thickness was sputtered on a transparent quartz substrate by a sputtering system (Balzers Cube) and protected by a SiO_2 thin film of 1 nm from oxidization. Here, the GST thin layer is defined in the amorphous state in our experiments. Subsequently, a 40 nm gold thin film was deposited onto the GST layer by e-beam evaporation (EB03 BOC, Edwards). The GST-Au hybrid samples were then spin-coated with a 500 nm thick layer of positive photoresist (S1805) and soft-baked at 75℃ for 1

#189457 - $15.00 USD Received 25 Apr 2013; revised 23 May 2013; accepted 25 May 2013; published 31 May 2013

minute. This temperature does not reach the crystalline temperature of the GST thin film. Therefore, the phase still remained in the amorphous phase which has been confirmed by comparing the transmission spectra before and after the soft baking process. Using the LIL technique [27], a square array of disk pattern with a lattice constant of 1.2 μm was generated on the photoresist layer. Then, the disks were trimmed to a uniform diameter of 280 nm via O_2 plasma processing. The photoresist pattern was transferred to the underlying gold layer via ion milling (RF-350, Veeco microetch). Figure 2(b) shows a scanning electron microscope (SEM) image of the fabricated gold nanodisks array. The fabricated gold nanodisks were in a large area of 0.8 × 0.8 cm^2 and covered by a 50 nm ZnS-SiO_2 capping layer in the last fabrication step. To characterize the fabricated samples, a UV-Vis-NIR spectrophotometer (SHIMADZU) was used to measure the transmission spectra. The phase transition of the GST phase-change thin film was carried out on a hotplate with a constant heating temperature of 135℃.

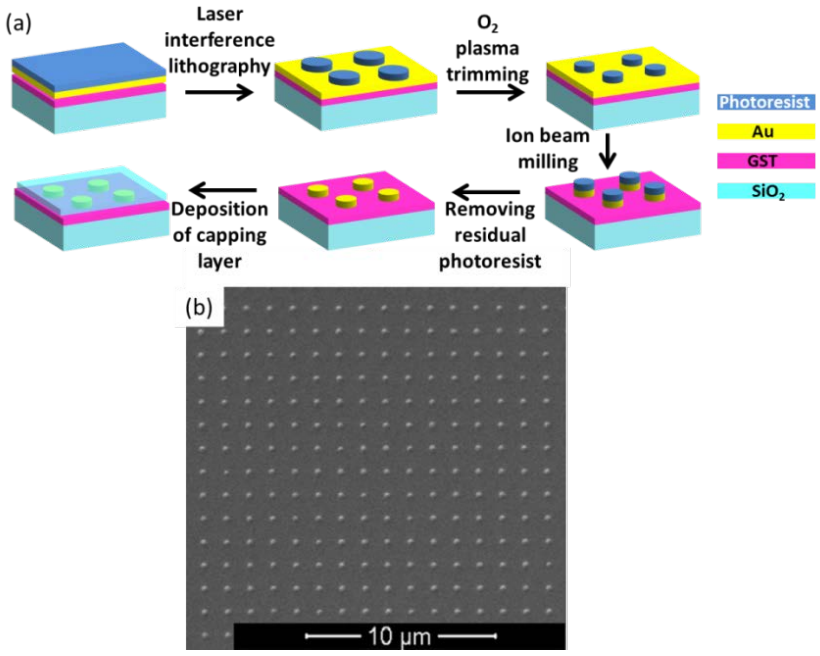

Fig. 2. (a) Schematic diagrams of the fabrication procedure. Laser interference lithography with etch-down process was used to fabricate the samples. (b) The SEM image of the fabricated gold nanodisk array before the deposition of the capping layer.

4. Evolution of the lattice resonance through the intermediate phases

In order to study the manipulation of the lattice resonance within the tuning range comprehensively, the fabricated hybrid phase-change plasmonic crystal with an amorphous GST thin film of 20 nm was crystallized at a temperature of 135℃ and the spectral measurements of the plasmonic crystal were taken every 5 minutes after rapidly cooling down the sample to room temperature. Several intermediate phases with different crystalline levels are revealed, accompanied with the lattice resonance shift in the range from 1.89 μm to 2.27μm. Figure 3(a) shows several measured transmission spectra of the hybrid plasmonic crystal at different intermediate phases. As anticipated, a red-shift of the lattice resonance is observed with an increasing baking time, indicating a more metal-like portion generated in the phase-change thin film. Large changes in the transmittance at a fixed wavelength are noticed via the intermediate phases, as demonstrated in Fig. 3(a) at 1.89 μm, the transmittance is 16% before baking (black curve), and increases to 72% after baking for 20 min (blue

#189457 - $15.00 USD Received 25 Apr 2013; revised 23 May 2013; accepted 25 May 2013; published 31 May 2013

curve). As, unlike VO_2 thin films used in phase transition, the phases of a GST thin film are stable at room temperature, the different intermediate states are non-volatile, suggesting opportunities in applications such as optical switches and nano-circuitry [28].

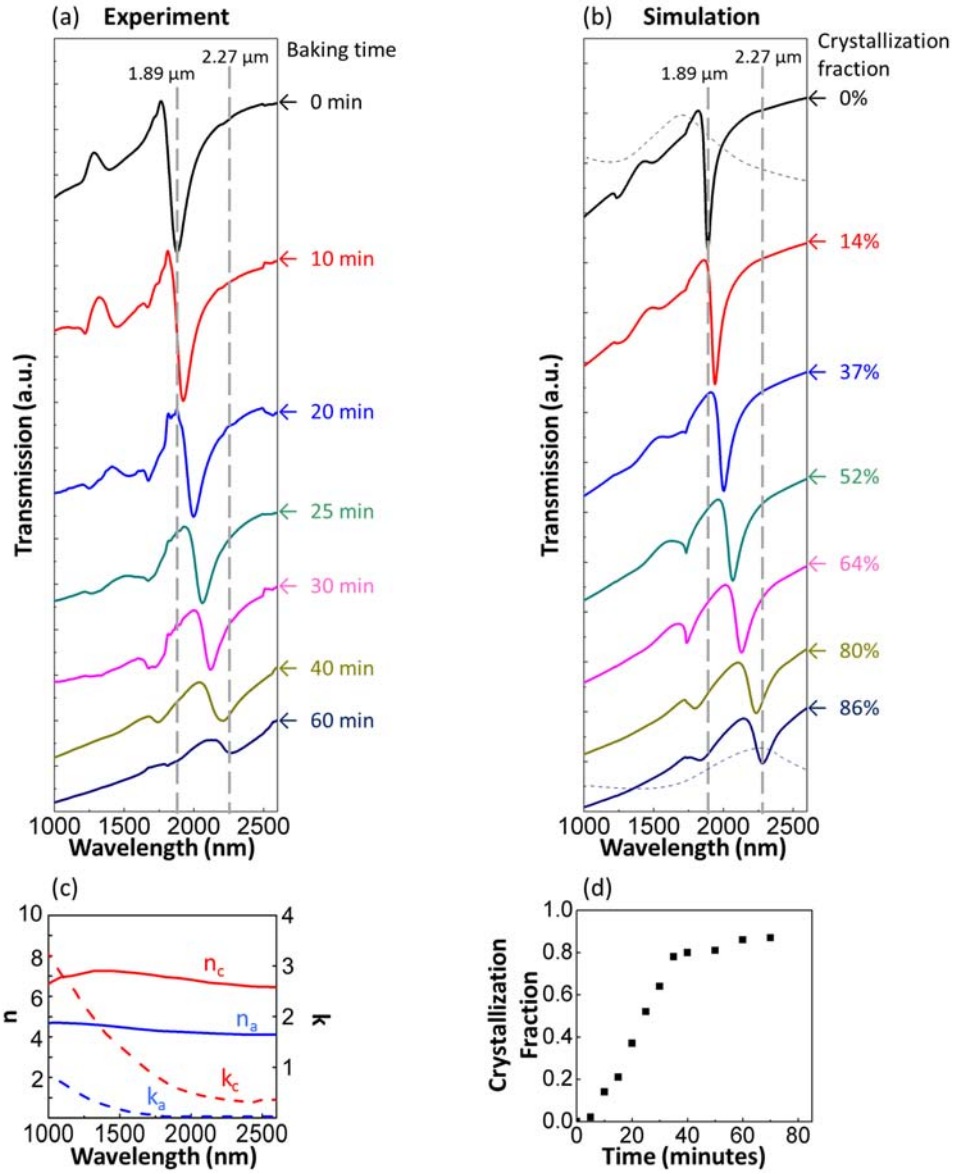

Fig. 3. (a) Experimental results of continuously tuning of the hybrid plasmonic crystals measured at different baking time during the crystallization process. (b) Simulation results of the hybrid plasmonic crystals with GST layer at the corresponding crystallization fraction to match the resonance shifts in the experiment. Dashed curves show the extinction cross-sections of a single unit cell at amorphous state (top) and 86% crystallized state (bottom). Experimental and simulation results are in good agreement, illustrating the evolution of the lattice resonance through intermediate states. (c) The optical constants of amorphous GST (n_a, k_a) and crystalline GST (n_c, k_c) [20]. Based on the resonance shifts in the transmission spectra, the relation between the crystallization fraction and crystallization time (d) is obtained.

Since GST is known as a nucleation-dominated material, many small crystalline nuclei are formed first when the temperature reaches its crystallization point and then numerous small

#189457 - $15.00 USD Received 25 Apr 2013; revised 23 May 2013; accepted 25 May 2013; published 31 May 2013

crystals are joined together to form a crystalline structure [29]. Thus, the fraction of the crystallized phase-change molecules in the GST thin layer can be estimated by corresponding spectral simulations. We assumed that the GST thin film in the intermediate phases is composed of different proportions of amorphous and crystalline molecules, and several effective-medium theories [30] can be applied to estimate the effective dielectric constant $\varepsilon_{eff}(\lambda)$ of such a GST thin film. In this work, the Lorentz-Lorenz relation [31] as defined by Eq. (1) is used for the approximation,

$$\frac{\varepsilon_{eff}(\lambda)-1}{\varepsilon_{eff}(\lambda)+2} = m \times \frac{\varepsilon_c(\lambda)-1}{\varepsilon_c(\lambda)+2} + (1-m) \times \frac{\varepsilon_a(\lambda)-1}{\varepsilon_a(\lambda)+2}, \quad (1)$$

where m denotes the crystallization fraction of the GST thin film ranging from 0 to 100%, $\varepsilon_c(\lambda)$ and $\varepsilon_a(\lambda)$ are the permittivity of GST in the crystalline and amorphous phases. The dielectric constant and refractive index are related by $\sqrt{\varepsilon(\lambda)} = n(\lambda) + ik(\lambda)$.

By careful selections of the value of m to match the resonance shifts, the corresponding simulated transmission spectra of the hybrid plasmonic crystals at different intermediate phases are shown in Fig. 3(b). The values of the refractive indices of GST in amorphous ($n_a(\lambda)$, $k_a(\lambda)$) and crystalline phases ($n_c(\lambda)$, $k_c(\lambda)$) are given in Fig. 3(c) [20]. Experimental and simulation results are in good agreement. The relation between the crystallization fraction and the heating and is plotted in Fig. 3(d). It can be seen that the crystallization rate is low at both the beginning and the end of crystallization process, while high in the middle region. This nonlinear relation is in good agreement with previous work [29]. Compared to the ideal cases in the simulation, the GST thin film can only be crystallized to a maximum of ~86% in our experimental apparatus as shown in Fig. 3(d). By extending the baking time, the transmission spectra do not show a further red-shift. Such a result may be due to the possible damage on the GST surface caused by ion milling during fabrication, and the way we heated the plasmonic crystal may also cause volume reduction of GST [32] as well as vacancy defects in the lattice so that GST cannot be entirely crystallized [33]. These problems can be alleviated by using non-destructive fabrication methods such as nanostencil lithography [34] and GST alloys prepared by other means [33,35].

The gradually widened and shallower resonance dip with an increasing crystalline level can be qualitatively explained by the refractive indices of amorphous and crystalline GST thin films. When the GST thin film is switched from the amorphous to crystalline phase, the increased extinction coefficient k associated with the crystallized GST indicates an intensity decrease of the localized surface plasmon resonance mode (LSPR) of each nanodisk. From the extinction cross-sections (the black and dark blue dashed curves) in Fig. 3(b), a more pronounced LSPR mode is generated when the GST thin film is in the amorphous phase. Regarding the real part of the refractive index n, its value is also increased with the crystallization fraction m and thus a larger refractive index mismatch occurs at the material interfaces. This increased mismatch, together with the increased extinction coefficient k, reduces the propagation length of the lattice surface mode [36]. As a result, the diffractive coupling is suppressed.

5. Conclusions

In summary, a hybrid plasmonic crystal consisted of a gold nanodisk array and an underneath GST phase-change thin film for the active tuning of lattice resonance has been demonstrated. By optimizing the thickness of the phase-change thin film, a hybrid plasmonic crystal with a GST thin film of 20 nm has been selected as an example to successfully show both in the simulations and experiments that the lattice resonance can be tuned in a wide range of around 500 nm. Also, such a resonance dip can be precisely tuned within this range by controlling different intermediate phases of the GST phase-change thin film. With the simulated spectra

#189457 - $15.00 USD Received 25 Apr 2013; revised 23 May 2013; accepted 25 May 2013; published 31 May 2013

corresponding to the experimental measurements, the dynamics of the crystallization process in a GST thin film has been investigated and the mechanism behind this tuning apparatus has been qualitatively explained. This modulation method based on the phase transition of the GST phase-change materials is fast, non-volatile at room temperature and capable to direct overwrite numerous cycles. To improve the tuning efficiency, energy-controlled light sources can be used to generate the multi-level optical states in the hybrid GST systems. The phase state of GST can be dynamically set to the designed values, making such devices applicable in the real-world. One challenge may need to be conquered is the energy loss in such a nanosystem. This work offers a platform for the future development of nanoscale optical modulators, switchers, sensors and nonlinear optical devices.

Acknowledgments

This work has been supported by the Engineering and Physical Sciences Research Council (APLAS project) and by the Leverhulme Trust. The authors would also like to acknowledge the funding provided by The Chinese Nature Science Grant (61138002) and Foundation of State Key Laboratory of Optical Technologies on Nano-Fabrication and Micro-Engineering.

#189457 - $15.00 USD Received 25 Apr 2013; revised 23 May 2013; accepted 25 May 2013; published 31 May 2013